



A New Method to Calculate the Fractal Dimension of Surfaces: Application to Human Cell Proliferation

Maxence Bigerelle, Alain Iost

► To cite this version:

Maxence Bigerelle, Alain Iost. A New Method to Calculate the Fractal Dimension of Surfaces: Application to Human Cell Proliferation. *Computers & Mathematics with Applications*, 2001, 42 (1-2), pp.241-253. 10.1016/S0898-1221(01)00148-1 . hal-04545533

HAL Id: hal-04545533

<https://hal.science/hal-04545533>

Submitted on 17 Apr 2024

HAL is a multi-disciplinary open access archive for the deposit and dissemination of scientific research documents, whether they are published or not. The documents may come from teaching and research institutions in France or abroad, or from public or private research centers.

L'archive ouverte pluridisciplinaire **HAL**, est destinée au dépôt et à la diffusion de documents scientifiques de niveau recherche, publiés ou non, émanant des établissements d'enseignement et de recherche français ou étrangers, des laboratoires publics ou privés.

A New Method to Calculate the Fractal Dimension of Surfaces: Application to Human Cell Proliferation

M. BIGERELLE AND A. IOST

Equipe Matériaux ENSAM Lille, Laboratoire de Métallurgie

Physique et Génie de Matériaux

CNRS UMR 8517, 8 Boulevard Louis XIV

59046 Lille CEDEX, France

Abstract—This paper presents a new method of calculating the fractal dimension of surfaces as well as a correction method which improved the results. To test its efficiency, the algorithms have been applied to stochastic surfaces of mathematical functions with known fractal dimensions and compared with the oscillation and the structure method. Better results have been found. This method, called ANAM, has been used to characterize the roughness of orthopaedic metallic substrates (Ti6Al4V alloy) in relation with human osteoblast adhesion. It has then been shown that the fractal dimension parameters correlated statistically with proliferation of cells, corresponding to a lower adhesion on less organized surfaces. The significant correlation observed between fractal dimension parameters and cell adhesion therefore adds a new concept to substratum roughness influence on cell behaviour.

Keywords—Fractal dimension, Surfaces, Numerical analysis, Human cells proliferation.

1. INTRODUCTION

Mandelbrot's work was all the more outstanding as it introduced the mathematical concept of fractal geometry in the field of sciences [1,2]. Since these papers, fractal analysis has been widely applied to account for physical phenomena like fracture, diffusion, fluid mechanics, and wear. The notion of the fractal dimension of a surface is related to its roughness: if the surface is smooth, it can be described by Euclidean geometry, and the dimension is $\Delta = 2$; if a surface is more tortuous, Δ is greater than two and tends to three when its irregularity becomes very high, i.e., the Euclidean dimension of a volume.

The dimension of a surface can be related to mechanical properties such as the fracture toughness [3] or the surface topography relative to machining or wear process [4], and a great deal of work has been recently done in this field. However, two conditions are needed before finding a physical interpretation of the obtained correlations. First, the method used to calculate the fractal dimension of a surface has to be validated by applying its algorithm to discretized surfaces

This work has been partially supported by the Federation of Biomaterials. We would like to thank K. Anselme from the IRMS (Research Skeleton Diseases Institute) for her cooperation on the biological part of this article.

obtained by functions where Δ is known. Second, the discretization procedure of the surfaces should not introduce artifacts such as noise or smoothing.

This paper is organized as follows: in Section 2, the definition of fractal dimension and classical methods used in literature to calculate Δ will be briefly reviewed. In Section 3, we present a new method to calculate the fractal dimension of a surface based on the properties of the seminorm functions L_α which is derived from the oscillation and structure methods introduced by Dubuc *et al.* [5]. This method is called “the average normalized autocorrelation method” (ANAM). In Section 4, we will talk about the errors due to the discretization process and introduce a correlation factor to improve the precision of the algorithms. The methods will then be applied and compared, in Section 5, with mathematical functions where the fractal dimensions are known. Finally, in Section 6, the algorithm will be used to compute fractal dimension of orthopaedic metallic substrates (Ti6Al4V) with various surface roughnesses, and the relation between fractal dimension and cell parameters will be analyzed.

2. THE USUAL METHOD TO CALCULATE THE FRACTAL DIMENSION

2.1. The Minkowski-Bouligand Dimension

Let E be a restricted part in \mathbb{R}^3 . Let $E(\tau)$ be the set of all points in \mathbb{R}^3 defined as follows:

$$E = \{(x, y, f(x, y)), a \leq x \leq b, c \leq y \leq d\} \text{ Graph of } f : [a, b] \times [c, d] \rightarrow \mathbb{R},$$

$$E(\tau) = \bigcup_{x, y \in E} B_\tau(x, y),$$

where $B_\tau(x)$ is an open disc of the Euclidean space with three dimensions centered on x and with a radius τ . The fractal dimension $\Delta(E)$ (or Minkowski-Bouligand dimension) of E is given by

$$\Delta(E) = \lim_{\tau \rightarrow 0} \left(3 - \frac{\log \text{vol } E(\tau)}{\log \tau} \right), \quad (1)$$

where $\text{vol } E(\tau)$ represents the volume—or the three-dimensional measure—of the Minkowski sausage.

2.2. Some Usual Methods to Calculate the Fractal Dimension

2.2.1. The oscillation method

This method was recently proposed by Dubuc *et al.* [5] and applied to roughness measurements of worn surfaces [6]. The τ -oscillation of the function f in x is defined as

$$f : [a, b] \times [c, d] \rightarrow \mathbb{R}, \quad \text{OSC}_\tau(f, x, y) = \left| \max_{\substack{|x-t| < \tau \\ |y-t| < \tau}} (f(t)) - \min_{\substack{|x-t| < \tau \\ |y-t| < \tau}} (f(t)) \right|; \quad (2)$$

by taking the average of $\text{OSC}_\tau(f, x, y)$ over the surface $[a, b] \times [c, d]$, we have

$$\text{VAR}_\tau(f, a, b, c, d) = \frac{1}{(b-a)} \frac{1}{(d-c)} \int_a^b \int_c^d \text{OSC}_\tau(f, x, y) dx dy, \quad (3)$$

and then the fractal dimension can be written

$$\Delta(f, a, b, c, d) = \lim_{\tau \rightarrow 0} \left(3 - \frac{\log \text{VAR}_\tau(f, a, b, c, d)}{\log \tau} \right). \quad (4)$$

$\Delta(f, a, b, c, d)$ is associated with the graph of function f defined over the square $[a, b] \times [c, d]$. With this method, the errors due to discretization on y disappear. It was shown [5,6] that this method is the most accurate to calculate the fractal dimension of functions $z = f(x, y)$. That is the reason why our method is based on the same background as the oscillation method.

2.2.2. The structure method

The structure function $s(f, \tau, a, b, c, d)$ may be defined as follows [7]. Let $a < b$, $c < d$, and f be a C^0 class function such as $f : [a - \tau, b + \tau] \times [c - \tau, d + \tau] \rightarrow \mathbb{R}$, $(x, y) \rightarrow f(x, y)$

$$s(f, \tau, a, b, c, d) = \int_a^b \int_c^d [f(x + \tau, y + \tau) - f(x - \tau, y - \tau)]^2 dx dy. \quad (5)$$

A modified representation which gives better results was proposed by Tricot [9] for profiles and could be extended to surfaces without difficulty

$$s_2(f, \tau, a, b, c, d) = \frac{1}{b-a} \frac{1}{d-c} \int_a^b \int_c^d \left[\frac{1}{\tau^2} \int_{u=x}^{u=x+\tau} \int_{v=y}^{v=y+\tau} [f(x, y) - f(u, v)]^2 du dv \right]^{1/2} dx dy; \quad (6)$$

then, fractal dimension is given by

$$\Delta(f, a, b, c, d) = \lim_{\tau \rightarrow 0} \left(3 - \frac{\log s_2(f, \tau, a, b, c, d)}{\log \tau} \right). \quad (7)$$

Despite the good results obtained by this function, it is rarely applied according to the other articles written on the subject.

3. A NEW ALGORITHM TO ESTIMATE THE FRACTAL DIMENSION OF A SURFACE

3.1. Description of the Method

Given four positive real numbers $a < b$, $c < d$, f is a C^0 class function such as $f : [a - \tau, b + \tau] \times [c - \tau, d + \tau] \rightarrow \mathbb{R}$, $x, y \rightarrow f(x, y)$. For a real number α , such as $\alpha \geq 1$, the function $L_\tau^\alpha(f, x, y)$ is defined by

$$L^\alpha[a, b] \times [c, d] = \left\{ f : [a, b] \times [c, d] \rightarrow \mathbb{R}; \int_c^d \int_a^b |f(x, y)|^\alpha dx dy < +\infty \right\}, \quad (8)$$

$$L_\tau^\alpha(f, x, y) = \left[\frac{1}{\tau^2} \int_0^\tau \int_0^\tau |f(x, y) - f(x - t_1, y - t_2)|^\alpha dt_1 dt_2 \right]^{1/\alpha}.$$

The above formulation implies an influence of the correlation between $f(x - t_1, y - t_2)$ and $f(x, y)$ on the calculation of $L_\tau^\alpha(f, x, y)$ and a variation inherent to the local autocorrelation of the function f .

This autocorrelation is minimized by taking the average of the local difference between the two functions over the whole interval τ , taking the function $M_\tau^\alpha(f, x, y)$ defined by

$$M_\tau^\alpha(f, x, y) = \left[\frac{1}{\tau^4} \int_{s_1=0}^\tau \int_{s_2=0}^\tau \int_{t_1=0}^\tau \int_{t_2=0}^\tau |f(x + s_1, y + t_1) - f(x - s_2, y - t_2)|^\alpha dt_2 dt_1 ds_2 ds_1 \right]^{1/\alpha}. \quad (9)$$

The function $K_\tau^\alpha(f, x, y)$ is defined by taking the average of $M_\tau^\alpha(f, x, y)$ over the whole interval $[a, b]$

$$K_\tau^\alpha(f, a, b, c, d) = \frac{1}{(b-a)(d-c)} \int_{x=a}^b \int_{y=c}^d M_\tau^\alpha(f, x, y) dx dy. \quad (10)$$

By making six times the average of the function, the variance of the estimation of $K_\tau^\alpha(f, a, b, c, d)$ diminishes faster than $\text{VAR}_\tau(f, a, b, c, d)$, $s(\tau, f, a, b, c, d)$, or $s_2(\tau, f, a, b, c, d)$ on the square $[a, b] \times [c, d]$. This method is called the surface average normalized autocorrelation method (SANAM).

3.2. Theorem

Let $H(f, a, b, c, d)$ (called the Hölder exponent) be a real such as $H(f, a, b, c, d) \in]0, 1]$, if f is uniformly Hölderian and satisfies the inequality $K_\tau^\alpha(f, a, b, c, d) \geq c' \tau^{H(f, a, b, c, d)}$ (c and c' are two positive real numbers); then for α , real, $\alpha \geq 1$,

$$c\tau^{H(f, a, b, c, d)} \geq K_\tau^\alpha(f, a, b, c, d) \geq c'\tau^{H(f, a, b, c, d)},$$

and

$$\Delta(f, a, b, c, d) = \lim_{\tau \rightarrow 0} \left(3 - \frac{\log K_\tau^\alpha(f, a, b, c, d)}{\log \tau} \right). \quad (11)$$

The fractal dimension is obtained by linear regression of $\log K_\tau^\alpha(f, a, b, c, d)$ versus $\log \tau$ for different τ values. The slope corresponds to the Hölder coefficient $H(f, a, b, c, d)$, and the fractal dimension is given by $\Delta(f, a, b, c, d) = 3 - H(f, a, b, c, d)$.

3.3. Demonstration

3.3.1. Theorems resorted to the demonstration

By extending Tricot's results [9] from profile to surface, it was shown that:

- (i) if f is Hölderian in (x, y) ($x \in [a, b]$, $y \in [c, d]$), there exists a constant c , depending on x and y , such that

$$\text{OSC}_\tau(f, x, y) \leq c\tau^{H(f, a, b, c, d)}; \quad (12)$$

- (ii) if the function f is uniformly Hölderian in (x, y) , there exists a constant c' , independent of x and y , such that

$$\text{VAR}_\tau(f, a, b, c, d) \leq c'\tau^{H(f, a, b, c, d)}, \quad \text{and then } \Delta(f, a, b) \leq 2 - H(f, a, b); \quad (13)$$

- (iii) if f is anti-Hölderian in (x, y) ($x \in [a, b]$, $y \in [c, d]$), there exists a constant $c > 0$, depending on (x, y) , such that

$$\text{OSC}_\tau(f, x, y) \geq c\tau^{H(f, a, b, c, d)}; \quad (14)$$

- (iv) if the function f is uniformly anti-Hölderian in (x, y) , there exists a constant c' , $c' > 0$, such that

$$\text{VAR}_\tau(f, a, b, c, d) \geq c'\tau^{H(f, a, b, c, d)}, \quad \text{and then } \Delta(f, a, b) \geq 2 - H(f, a, b). \quad (15)$$

3.3.2. Lemma 1

STATEMENT.

$$\forall \alpha \geq 1, \quad M_\tau^\alpha(f, x, y) \leq \text{OSC}_\tau(f, x, y), \quad (16)$$

$$\forall \alpha \geq 1, \quad K_\tau^\alpha(f, a, b, c, d) \leq \text{VAR}_\tau(f, a, b, c, d). \quad (17)$$

PROOF. Using four times the mean theorem on (9), we obtain $\exists \{s_1^0, s_2^0, t_1^0, t_2^0\} \in [0, \tau]$ such that $M_\tau^\alpha(f, x, y) = |f(x + s_1^0, y + t_1^0) - f(x - s_2^0, y + t_1^0)|^\alpha$, as $|f(x + s_1^0, y + t_1^0) - f(x - s_2^0, y + t_2^0)| \leq \text{OSC}_\tau(f, x, y)$, and leads to (16). By integrating (16) on the square $[a, b] \times [c, d]$, (17) is found.

3.3.3. Lemma 2

STATEMENT. If f is uniformly Hölderian over the whole surface $[a, b] \times [c, d]$, then

$$K_\tau^\alpha(f, a, b, c, d) \leq c\tau^{H(f, a, b, c, d)}, \quad \text{and } \Delta(f, a, b, c, d) \leq 3 - H(f, a, b, c, d). \quad (18)$$

PROOF. If f is uniformly Hölderian, therefore from (17) and (13), one gets $K_\tau^\alpha(f, a, b, c, d) \leq c\tau^{H(f, a, b, c, d)}$ and then $\Delta(f, a, b, c, d) \leq 3 - H(f, a, b, c, d)$. From (4) and (17), the following relation can be inferred:

$$\Delta(f, a, b, c, d) \geq \lim_{\tau \rightarrow 0} \left(3 - \frac{\log K_\tau^\alpha(f, a, b, c, d)}{\log \tau} \right). \quad (19)$$

3.3.4. Lemma 3

STATEMENT. If f satisfies on the whole interval $[a, b]$

$$K_\tau^\alpha(f, a, b, c, d) \geq c'\tau^{H(f, a, b, c, d)}, \quad (20)$$

then f is uniformly anti-Hölderian over the whole interval $[a, b]$, and under the conditions defined in Lemma 2, one obtains

$$c\tau^{H(f, a, b, c, d)} \geq K_\tau^\alpha(f, a, b, c, d) \geq c'\tau^{H(f, a, b, c, d)}, \quad \text{and } \Delta(f, a, b, c, d) = 3 - H(f, a, b, c, d). \quad (21)$$

PROOF. As (17) is always true, one gets $\text{VAR}_\tau(f, a, b, c, d) \geq K_\tau^\alpha(f, a, b, c, d) \geq c'\tau^{H(f, a, b, c, d)}$; then f is uniformly anti-Hölderian over the whole interval $[a, b] \times [c, d]$. From (15), $\Delta(f, a, b, c, d) \geq 3 - H(f, a, b, c, d)$, and with the same statement as for Lemma 2, one obtains

$$\Delta(f, a, b, c, d) \leq \lim_{\tau \rightarrow 0} \left(3 - \frac{\log K_\tau^\alpha(f, a, b, c, d)}{\log \tau} \right),$$

and under the conditions defined in Lemma 2, (21) is found.

REMARK. A great number of fractals functions such as Weierstrass [8] or Knopp [6] satisfies (21).

4. NUMERICAL COMPUTATION

4.1. Discretization

In order to discretize equation (10) by numerical method, first-order numerical integration is used, which gives a good evaluation of $K_\tau^\alpha(f, a, b, c, d)$ with less consuming calculation time. The problem of the borders—as in other methods—must now be considered. In fact, if the function f is defined over the surface $[a, b] \times [c, d]$, it is impossible to perform the calculation if $x \in [b - \tau, b]$, $x \in [a, a + \tau]$, $y \in [d - \tau, d]$, or $y \in [c, c + \tau]$. To avoid introducing a bias in the calculation, the integration of $K_\tau^\alpha(f, a, b, c, d)$ is carried out over the interval $[a + \tau, b - \tau] \times [c + \tau, d - \tau]$ (that is to say that $K_\tau^\alpha(f, a, b, c, d)$ will depend on the number of discretized points).

Let us define by $(x_1, y_1, f_{1,1}), (x_2, y_1, f_{2,1}), \dots, (x_n, y_p, f_{n,p})$ the discretization points of the graph $f(x_i - x_{i-1} = \delta, y_i - y_{i-1} = \delta, i \in [2, n])$. This sixth integral is a sixth mean on the discretization points regarding six variables, since k is the number of elementary segments with length δ that can be found in the window with width τ ($\tau = k\delta$), n is the number of discretized points from the graph of the function f , and $K_\tau^\alpha(f, a, b, c, d)$ is averaged on $(n - 2k)^2$ points. Finally, the formula used for calculation is then obtained

$$K_{\tau=k\delta}^\alpha(f, n) = \frac{(k+1)^{-4/\alpha}}{(n-2k)^2} \sum_{i=k+1}^{n-k} \sum_{j=k+1}^{n-k} \left[\sum_{m=0}^k \sum_{n=0}^k \sum_{q=0}^k \sum_{p=0}^k |f_{i+m, j+n} - f_{i-q, j-p}|^\alpha \right]^{1/\alpha}. \quad (22)$$

Under hypothesis (21), the graph of the variation of $\log(k\delta)$ versus $K_{\tau=k\delta}^\alpha(f, n)$ is a straight line, where the slope is the Hölder exponent.

4.2. Discretizing Errors

To calculate the fractal dimension of a surface by numerical calculation, the surface must first be discretized in a finite number of points. If the surface is derivative (except eventually on a set of points), there are theorems which allow us to estimate the error made by discretizing the function. The algorithms derived from these theorems are based on the derivation of the functions. Conversely, the function of a fractal surface is generally not derivable over the definition interval, and it is then difficult to estimate the error made in some mathematical measures derived from discretization assumptions. We have proved [10] that numerical function used to estimate fractal dimension (oscillation, AMN, structure) underestimate the true values, particularly for high fractal dimensions. Then, a correction method has been proposed [4] to quantify these errors,

$$\text{Surf}_\tau(f, a, b, c, d) = \eta\tau^{H(f, a, b, c, d)} + \sum_{i=1}^p \frac{e_i}{\tau^i}. \quad (23)$$

$H(f, a, b, c, d)$, α , e_i can be obtained by minimizing (23), and the problem is solved by nonlinear regression. In fact, there are no mathematical reasons, except for the discretization phenomenon, so that $\text{Surf}_\tau(f, a, b, c, d)$ is a function with terms $1/\tau^i$. By statistical analysis, we take the coefficient e_i only if its value is significantly different from 0 (Student's test). Moreover, using the nonlinear regression, it can be proved that $d\tau^{H(f, a, b, c, d)}$ and e_i/τ are orthogonal by regression; by adding the term e_i/τ in the regression model, the expectation of $H(f, a, b, c, d)$ is unchanged.

The method presented to estimate the errors due to discretization is justified for the variation method and can be applied to the ANAM method introduced in Section 3. This method is called the corrected normalized autocorrelation method (CANAM).

4.3. Discretization on Experimental Surfaces

To calculate the fractal dimension from (22), the discretization sample on the x -axis (δ_x) has to be identical to that of the y -axis (δ_y). Since some experimental surfaces (obtained, for example, by profilometers) can possess different numbers of discretization points between the x - or y -axes, then the following equation can be used:

$$K_{\tau=k_x\delta_x, \tau=k_y\delta_y}^\alpha(f, n_y, n_x) = \frac{(k_x + 1)^{-2/\alpha}(k_y + 1)^{-2/\alpha}}{(n_x - 2k_x)(n_y - 2k_y)} \sum_{i=k_x+1}^{n_x-k_x} \sum_{j=k_y+1}^{n_y-k_y} \left[\sum_{m=0}^{k_x} \sum_{n=0}^{k_y} \sum_{q=0}^{k_x} \sum_{p=0}^{k_y} |f_{i+m, j+n} - f_{i-q, j-p}|^\alpha \right]^{1/\alpha}, \quad (24)$$

where

- δ_x and δ_y are sampling length on the x - and y -axes,
- n_x and n_y are the numbers of discretization points of the surface, and
- k_x and k_y are the numbers of points used to calculate the K functions with $\tau = k_x\delta_x$ and $\tau = k_y\delta_y$.

Relations $\tau = k_x\delta_x$ and $\tau = k_y\delta_y$ must be respected to apply this method, and the experimenter must find the different τ values which satisfy these relations.

5. NUMERICAL VALIDATION

We have proposed to validate our algorithm making a comparison with the structure and variation method when applied to mathematical surfaces with a given fractal dimension.

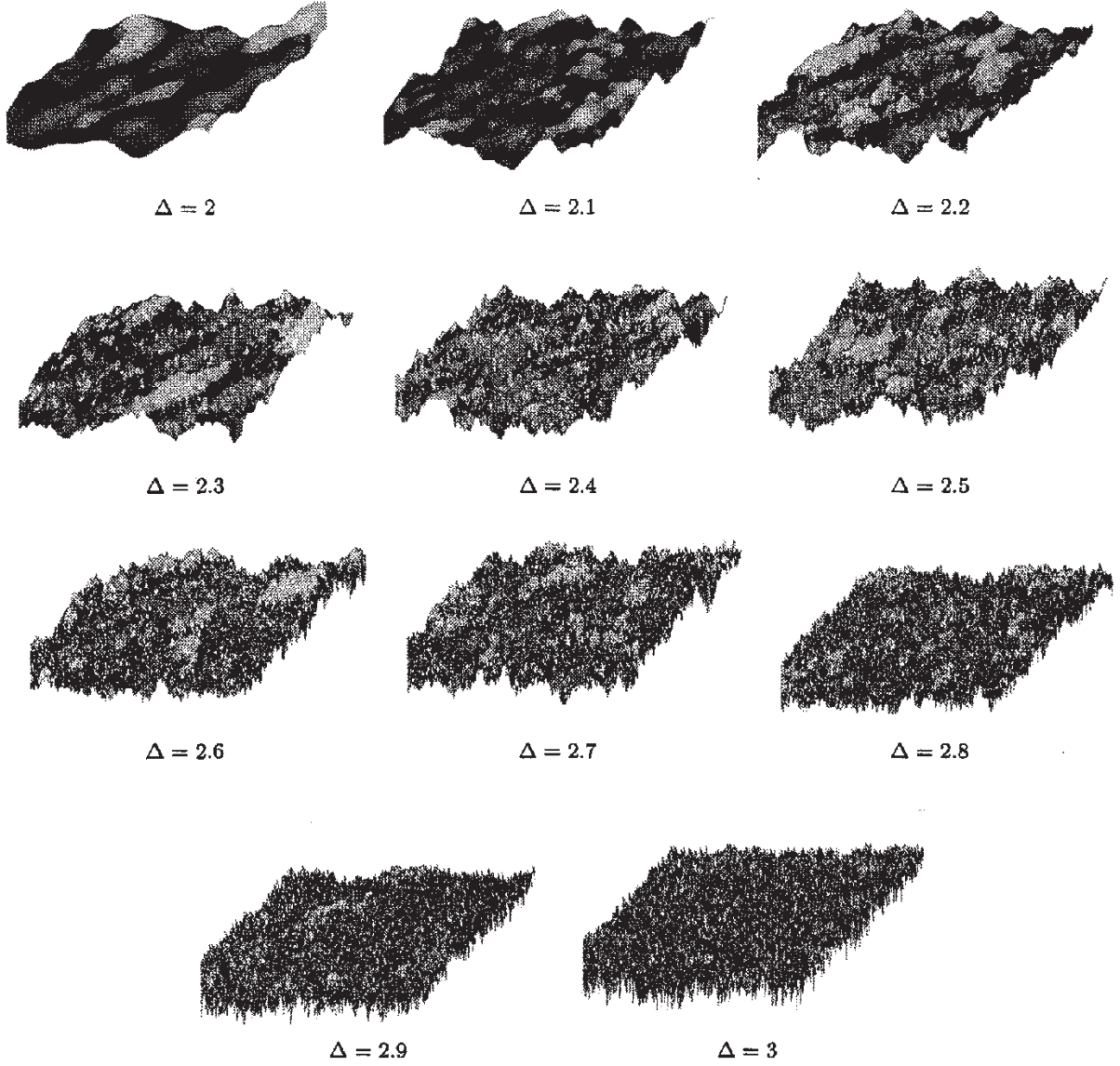


Figure 1. Weierstrass surfaces with fractal dimensions varying from two to three. Curves are discretized in a grid of 2048×2048 points.

5.1. Fractal Surfaces

• The Weierstrass surfaces

Three-dimensional fractal Weierstrass surfaces are defined by [8]

$$W(x, y) = A \sum_{n_1=0}^{\infty} \sum_{n_2=0}^{\infty} a_{n_1 n_2} \frac{\gamma^{(n_1+n_2)/2}}{[\gamma^{2n_1} + \gamma^{2n_2}]^{(H+1)/2}} \cos(2\pi\gamma^{n_1} + \varphi_{n_1 n_2}) \cos(2\pi\gamma^{n_2} + \Psi_{n_1 n_2}), \quad (25)$$

where $\varphi_{n_1 n_2}$ and $\Psi_{n_1 n_2}$ are stochastic phases of uniform density defined in $[0, 2\pi]$. A is a scale coefficient, $a_{n_1 n_2}$ are normal random numbers, H is the Hölder exponent ($H \in [0, 1]$), and γ is the frequency of the function with $\gamma > 1$. The functions plotting for fractal dimension $\Delta = (2, \dots, 3)$ are shown in Figure 1, and their associated surface responses are plotted in Figure 2.

• The Brownian surfaces

Mandelbrot [1] proposed creating a surface of fractal dimension 2.5 by the process described below: we first consider a plane. A random linear plot belongs to the plane. A part of the

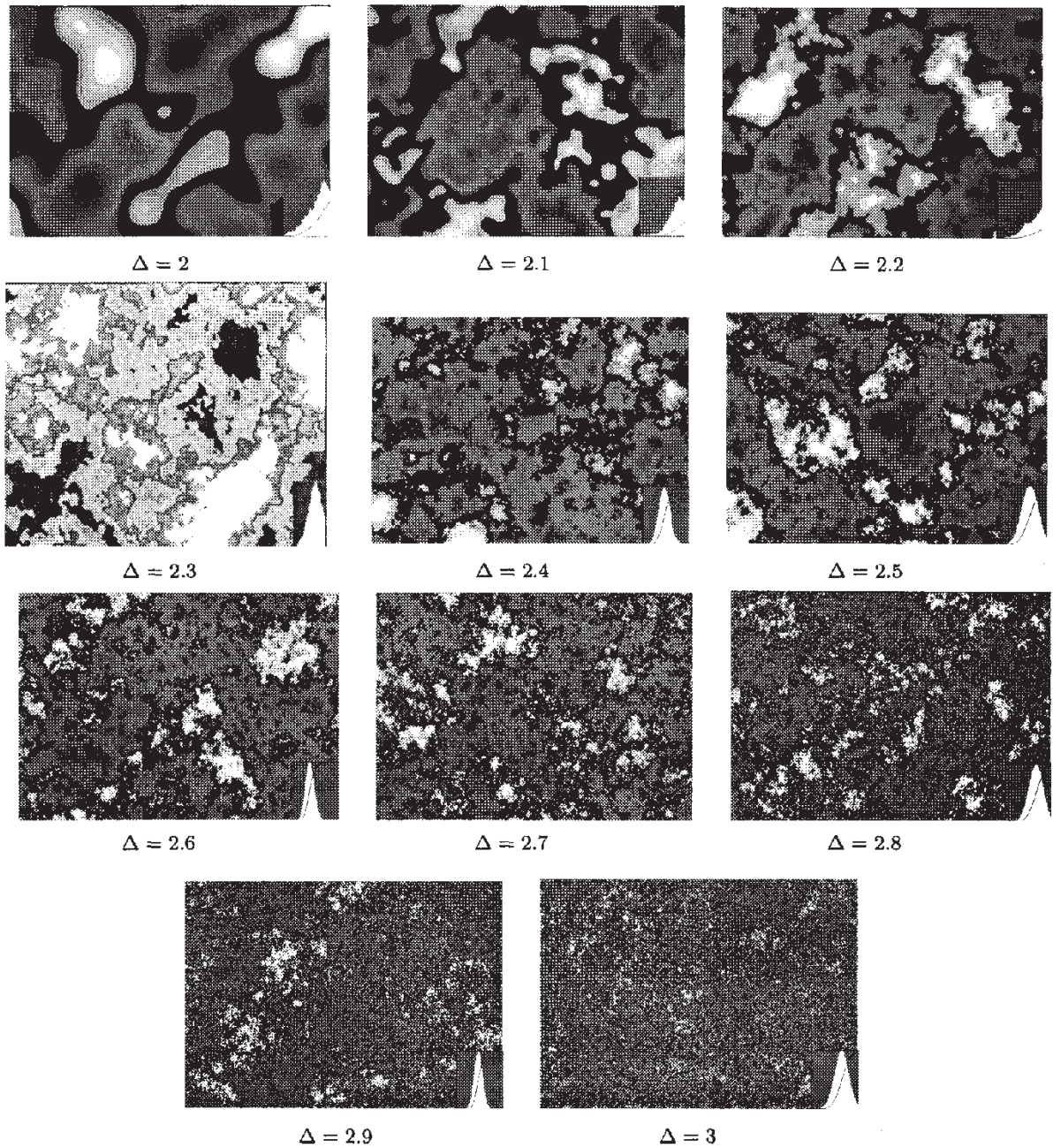


Figure 2. Surface response of the Weierstrass surfaces plot in Figure 1.

plane delimited by this linear plot is randomly dropped. Repeating this operation leads to the construction of a stochastic surface, as shown in Figure 3b.

Then, two other surfaces are used:

- a three-dimensional sinusoid with random phases and amplitudes ($\Delta = 2$) (Figure 3a), and
- a white noise surface ($\Delta = 3$) (Figure 3c).

5.2. Computational Results

The efficiency of the ANAM method and of the correction factor applied to different methods is shown in Figure 4 for Weierstrass function. As the fractal dimension rises, the risk of error in discretizing becomes more important, and the corrections corresponding to (23) are most efficient. These corrections improve all the methods (structure, oscillation, ANAM) which underestimate the fractal dimension. This is due to error in estimating the functions (3), (5), or (6) that are minimized for a small number of points (lower τ) and particularly for high fractal dimension.

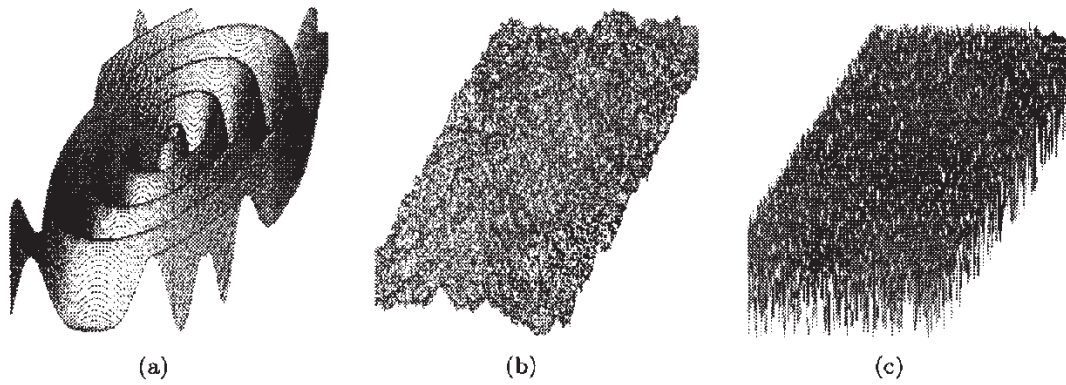


Figure 3. Plot of the sinusoid (a), Brownian (b), and white noise (c) surfaces discretized on a grid of 2048×2048 points.

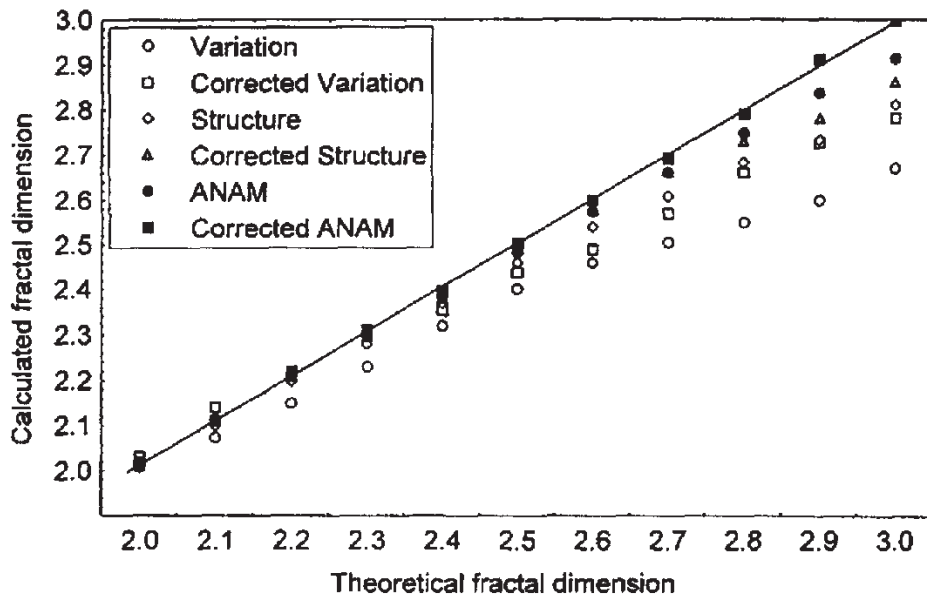


Figure 4. Plot of the calculated fractal dimension of the stochastic Weierstrass surfaces versus the theoretical one using the variation, structure, and ANAM algorithm with or without correction.

However, ANAM performed a double means rather than a difference in the τ -square that increases the precision of the evaluation of the fractal dimension. Using the ANAM with correction, errors are less than 1% for all the theoretical fractal dimension. Results obtained from the sinusoid, Brownian surface, and noise surface, reported in Table 1, confirm our analyses.

Table 1. Values of the fractal dimension for sinusoid, Brownian surface, and a noisy surface calculated by the oscillation, structure, and ANAM methods with or without correction by (23).

	Sinusoid $\Delta = 2$		Brownian $\Delta = 2.5$		Noise $\Delta = 3$	
	Normal	Corrected	Normal	Corrected	Normal	Corrected
Oscillation	2.06	2.06	2.32	2.38	2.58	2.79
Structure	2.05	2.06	2.34	2.39	2.70	2.82
ANAM	2.06	2.05	2.44	2.48	2.85	2.98

6. A BIOLOGICAL APPLICATION: HUMAN CELL ADHESION ON TITANIUM ALLOYS

We proposed to apply the ANAM methods to quantify the influence of the fractal aspect of surfaces on which human cells adhere and to connect it to the properties of some human biological cells.

6.1. Purpose of Study

Quantitatively, human osteoblasts adhesion on metallic substrates (Ti6A14V alloy) with various surface roughnesses is studied for several delays after inoculation and is correlated with qualitative modifications in the expression of protein adhesion, proteins expression, and with parameters describing the topography of surfaces in an extended way. Cell adhesion is a fundamental process directly involved in cell growth, cell migration, and cell differentiation. Adhesion is implied in embryogenesis, maintenance of tissue integrity, wound healing, immune response, cancer metastasis, and biomaterial tissue integration [11–14]. We propose to develop an evaluation of human osteoblast adhesion and to correlate the quantitative results obtained with parameters giving an extensive description of orthopaedic metallic surfaces (Ti6A14V alloy) with various roughnesses.

6.2. Experimental Procedure

180 discs of a Ti6A14V-ELI alloy (medical quality) 14 mm in diameter and 2 mm in height were processed by sandblasting (500 μm or 3 mm alumina particles) or by mechanical polishing (with P4000, P1200, or P80 silicon carbide paper). 36 discs for each treatment were prepared on which six three-dimensional surfaces have been measured using a confocal microscope laser (Lasertec). Discretizing the three-dimensional surfaces gives a scanning surface of 60 μm^2 . Surfaces have been straightened up using the least squares method without filtering to analyze surface topographies. The fractal dimensions have been computed using the ANAM method. Figure 5a represents the surfaces of the p80 polished ($\Delta = 2.23 \pm 0.02$) and the 3 mm sandblasted surface ($\Delta = 2.47 \pm 0.02$). Then, human bone cells obtained from the trabecular bone from the iliac crest of a nine year-old patient have been deposited on this substrate. Thirty samples of each surface have been inoculated with 2×10^4 cells/sample. Five samples have been analyzed after the following incubation period: 24 hours, 3 days, 7 days, 14 days and 21 days.

6.3. Relation between Fractal Dimension and the Cell Organizations

The higher the fractal dimension is, the more disorganized the surface appears (Figure 5a). At first the cell morphology is analyzed:

- Figure 5b represents the human cells osteoblast on the TA6V samples. For the polished surface, a confluent cell layer covered the samples. Cells appeared flattened and oriented in a parallel way. On the sandblasted surface, cells have a stellate shape with numerous filamentous extensions.
- Figure 5c represents the F-Actine of the osteoblast that characterized the organization of the cytoskeleton. On smooth surfaces, the cell skeleton is well organized with parallel fiber, but for the sandblasted one, the skeleton is disorganized.
- The antivinculin (Figure 5d) revealed the focal points of the cells and illustrated the distribution of the points of cell adhesion. For the polished surface, focal points are uniformly distributed, but for the sandblasted surface, they are visible on the extremities of the cells.
- The collagen expression (Figure 5e) describes the cell orientation.

For the polished surface, cells appear organized, while for the sandblasted one, the cell orientation is hazardous. These experiments show that the biological cell organization on TA6V substrate depends on the disorder of the surface.

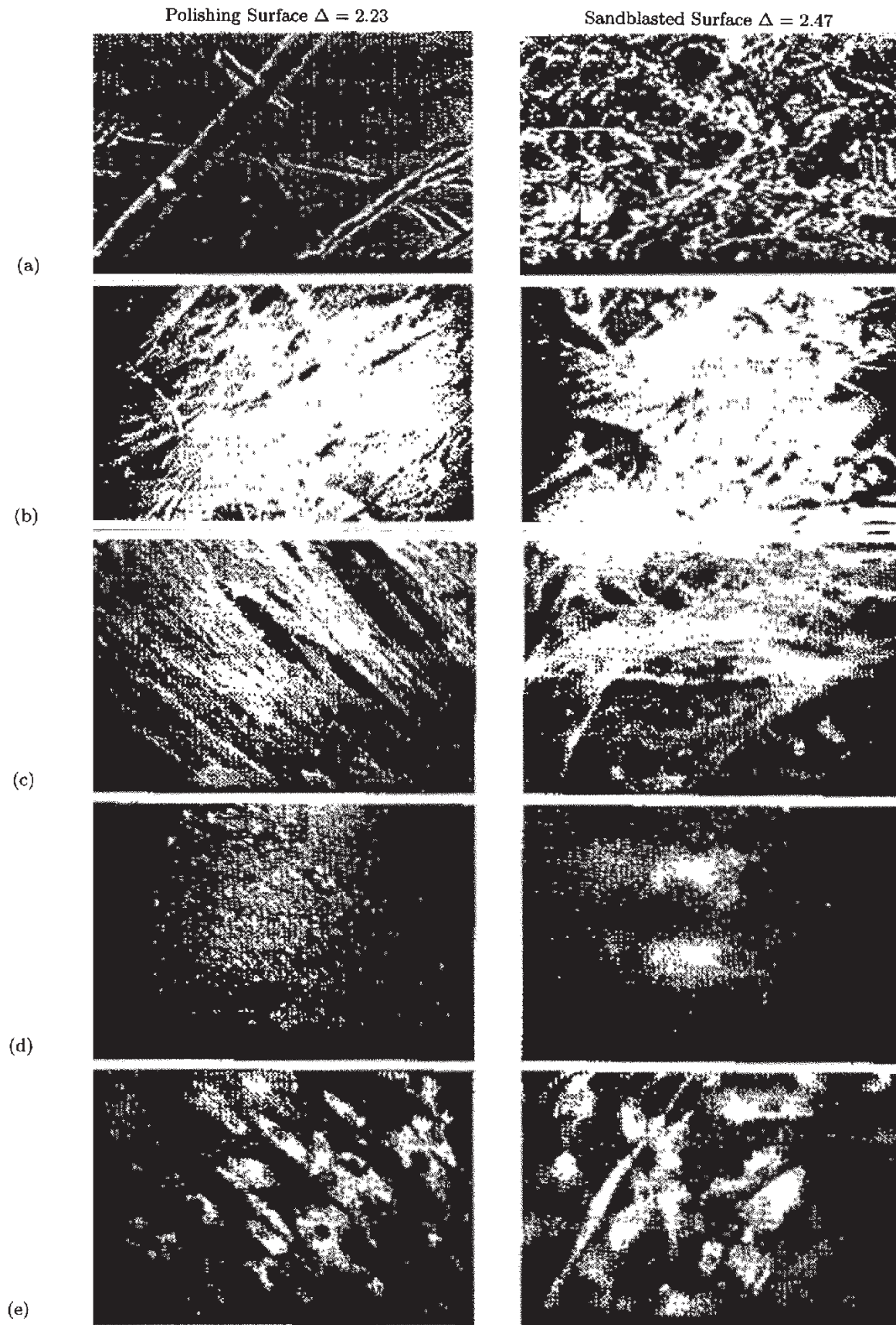


Figure 5. Left: Sample polished by p80 SiC disk ($\Delta = 2.23$). Right: the sandblasted one ($\Delta = 2.47$). (a) initial surface; (b) human cells osteoblast; (c) the F-Actine of the osteoblast (organization of the cytoskeleton); (d) the antivinculin illustrate (distribution of point of cell adhesion); (e) the collagen expression (cell orientation).

6.4. Modelization of Cell Proliferation

We analyzed the cell proliferation versus time and the fractal dimension of all the surfaces. We then postulated that cell proliferation could be modeled by the following equation:

$$P(t, \Delta) = \frac{\beta_1(\Delta - 2)H(t, t_0) + \beta_2}{1 + \exp[\beta_3(t - t_0) + \beta_4]}, \quad (26)$$

where t_0 is the time of the first cell count after cell deposition and $H(t, t_0)$ a heavyside function with $H(t, t_0) = 0$ if $t = t_0$ else $H(t, t_0) = 1$. Using a nonlinear least square method, the following coefficients are obtained with their asymptotic standard errors:

$$\beta_1 = -300000 \pm 30000, \quad \beta_2 = 180000 \pm 12000, \quad \beta_3 = -0.30 \pm 0.03, \quad \text{and} \quad \beta_4 = 2.76 \pm 0.2.$$

All coefficients are highly significant so that this model well describes the cell proliferation and gives a good accuracy with the experimental data corresponding to a correlation coefficient of 0.98 (Figure 6). When fractal dimension increases, the kinetics of cell proliferation decreases.

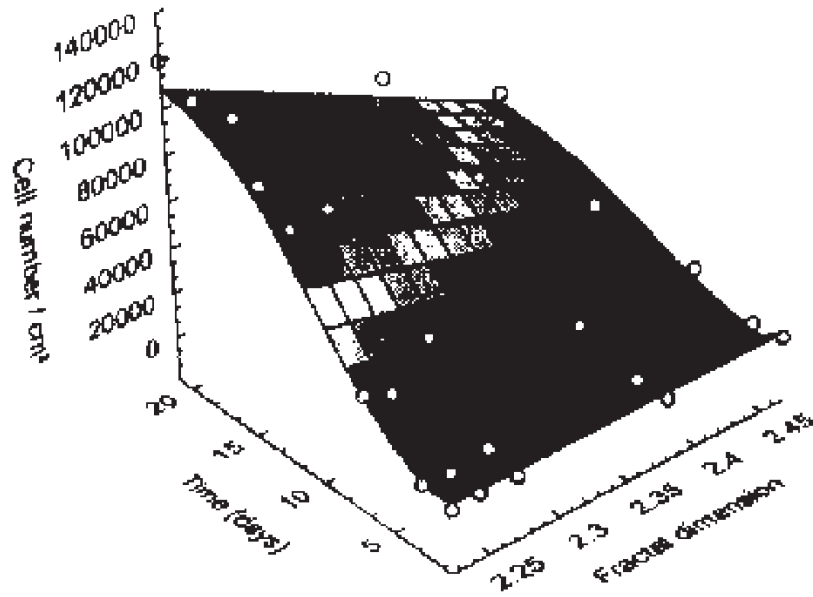


Figure 6. Cell proliferation versus time in culture and the fractal dimension. The surface response represents the model given by (26), and points are experimental data.

7. CONCLUSION

In conclusion, a new method called ANAM is presented to calculate the fractal dimension of surfaces. A correction factor is introduced which improves both our results, and those obtained by other methods. This method entails supposed that the investigated surface is both Hölderian and anti-Hölderian. With experimental surface, this condition cannot be verified, but this hypothesis is not strong enough to apply ANAM method on experimental curves. Results are correct when the ANAM method is used both on smooth and chaotic surfaces. This method, which consists of calculating the fractal dimension, does not require that surfaces should be self-similar or self-affine. There are other methods to calculate fractal dimension which require only the validation of one of these two conditions. So, ANAM method could be complementary with another method when the surface cannot be considered as not self-similar or self-affine. In fact, it is possible to decrease the calculation time of our method by avoiding evaluating redundant operations. The fractal dimension becomes a parameter that characterizes the disorder of the surface and can be applied to correlate the influence of the chaotic aspect of the surface with physical responses. Application to the human cell adhesion on TA6V substrates with different roughnesses shows that proliferation decreases when the fractal dimension increases.

REFERENCES

1. B.B. Mandelbrot, *The Fractal Geometry of Nature*, W.H. Freeman and Company, New York, (1983).
2. B.B. Mandelbrot, *Les Objects Fractals*, Flammarion, Paris, (1975).
3. E. Charkaluk, M. Bigerelle and A. Iost, Fractal and fracture, *Engen. Fract. Mech.* **61**, 119–139, (1998).
4. M. Bigerelle, Caractérisations géométriques de surfaces et interfaces, Applications des fractales en métallurgie, Thesis, ENSAM, Lille (1999).
5. B. Dubuc, J.F. Quiniou, C. Roques-Carnes, C. Tricot and S.W. Zucker, Evaluating the fractal dimension of profiles, *Phys. Rev.* **A39**, 1500–1512, (1989).
6. C. Tricot, P. Ferland and G. Baran, Fractal analysis of worn surfaces, *Wear* **172**, 127–133, (1994).
7. D. Whebi, Approche fractale de la rugosité des surfaces et implication analytique, Thesis, Besançon, (1986).
8. J. Lopez, G. Hansali, J.C. Le Bossa and T. Mathia, Caractérisation fractale de la rugosité tridimensionnelle d'une surface, *J. Phys. III France* **4** **42**, 2501–2519, (1994).
9. C. Tricot, *Courbes et Dimension Fractale*, Springer-Verlag, Paris, (1993).
10. E. Charkaluk, M. Bigerelle and A. Iost, Characterization of rough surfaces, *Proceedings of the 4th European Conference on Advanced Materials and Processes EUROMAT'95, Venice*, 511–515, (1995).
11. A. Naji and M.F. Harmand, Study of the effect of the surface state on the cytocompatibility of a Co-Cr alloy using human osteoblasts and fibroblasts, *J. Biomed. Mat. Res.* **24**, 861–871, (1990).
12. M. Könönen, M. Hornia, J. Kivilahti, J. Hautaniemi and I. Thesleff, Effect of surface processing on the attachment, orientation, and proliferation of human gingival fibroblasts on titanium, *J. Biomed. Mat. Res.* **26**, 1325–1341, (1992).
13. D.W. Murray, T. Rae and N. Rushton, The influence of the surface energy and roughness of implants on bone resorption, *J. Bone Joint Surg.* **71-B**, 632–637, (1989).
14. U. Meyer, D.H. Szulczewski, K. Möller, H. Heide and D.B. Jones, Attachment kinetics and differentiation of osteoblasts on different biomaterials, *Cells and Materials* **3**, 129–140, (1993).